available at www.sciencedirect.com

ScienceDirect

journal homepage: www.elsevier.com/locate/biochempharm

Acetaminophen normalizes glucose homeostasis in mouse models for diabetes

Howard G. Shertzer [a,*], *Scott N. Schneider* [a], *Eric L. Kendig* [a], *Deborah J. Clegg* [b], *David A. D'Alessio* [c], *Mary Beth Genter* [a]

[a] *Department of Environmental Health and Center for Environmental Genetics, University of Cincinnati Medical Center, Cincinnati, OH 45267, USA*

[b] *Department of Psychiatry, Center for Obesity Research, University of Cincinnati Medical Center, Cincinnati, OH 45267, USA*

[c] *Department of Medicine, Division of Endocrinology, Diabetes and Metabolism, University of Cincinnati Medical Center, Cincinnati, OH 45267, USA*

ARTICLE INFO

Article history:
Received 19 October 2007
Accepted 6 December 2007

Keywords:
Acetaminophen
Glucose control
Insulin resistance
Oxidative stress
Type 1 and type 2 diabetes

ABSTRACT

Loss of pancreatic beta cell insulin secretion is the most important element in the progression of type 1 and type 2 diabetes. Since oxidative stress is involved in the progressive loss of beta cell function, we evaluated the potential for the over-the-counter analgesic drug and antioxidant, acetaminophen (APAP), to intervene in the diabetogenic process. We used mouse models for type 1 diabetes (streptozotocin) and type 2 diabetes (high-fat diet) to examine the ability of APAP to intervene in the progression of diabetes. In C57BL/6J mice, streptozotocin caused a dosage dependent increase in fasting blood glucose (FBG), from 100 to >600 mg/dl. Daily APAP (20 mg/kg BW, gastric gavage), significantly prevented and partially reversed the increase in FBG levels produced by streptozotocin. After 10 weeks on a high-fat diet, mice developed fasting hyperinsulemia and impaired glucose tolerance compared to animals fed a control diet. APAP largely prevented these changes in insulin and glucose tolerance. Furthermore, APAP prevented most of the increase in body fat in mice fed the high-fat diet. One protective mechanism for APAP is suggested by studies using isolated liver mitochondria, where low micromolar concentrations abolished the production of reactive oxygen that might otherwise contribute to the destruction of pancreatic β-cells. These findings suggest that administration of APAP to mice, in a dosage used safely by humans, reduces the production of mitochondrial reactive oxygen and concomitantly prevents the development of type 1 and type 2 diabetes in established animal models.

1. Introduction

Obesity and diabetes are at epidemic proportions in American and Western populations [1]. Type 1 diabetes (previously termed juvenile onset diabetes) the most common chronic metabolic disease of childhood, results from an autoimmune-mediated loss of pancreatic islet β-cell mass. Type 2 diabetes (previously termed adult onset diabetes) usually

* *Corresponding author* at: Department of Environmental Health, University of Cincinnati College of Medicine, 3223 Eden Avenue, Cincinnati, OH 45267-0056, USA. Tel.: +1 513 558 0522; fax: +1 513 558 0925.
E-mail address: shertzhg@ucmail.uc.edu (H.G. Shertzer).

Abbreviations: APAP, acetaminophen (N-(4-hydroxyphenyl)acetamide); FBG, fasting blood glucose; STZ, streptozotocin (1-methyl-1-nitroso-3-[2,4,5-trihydroxy-6-(hydroxymethyl)oxan-3-yl]-urea); T1DM, type 1 diabetes mellitus; T2DM, type 2 diabetes mellitus.

0006-2952/$ – see front matter © 2007 Elsevier Inc. All rights reserved.
doi:10.1016/j.bcp.2007.12.003

occurs later in life and is typically preceded by obesity and associated metabolic abnormalities such as insulin resistance and dyslipidemia. Obesity is a primary risk factor for type 2 diabetes. Estimated U.S. costs for health care related to obesity are about $117 billion per year [2] and the years of life lost to obesity in the United States were estimated at 13–20 for males and 5–8 for females [3] In humans, a collection of conditions (elevated fasting blood insulin levels, glucose intolerance, an increase in abdominal fat, body mass index and blood lipid levels) is often termed metabolic syndrome [4,5]. The condition may be thought of as a cluster of risk factors for type 2 diabetes, or simply a prediabetic state. Weight loss may delay or prevent the onset of type 2 diabetes in obese individuals having impaired glucose tolerance, and even lessen the severity of insulin resistance [6,7]. Despite the growth of diabetes into one of the major causes of mortality, morbidity and health care expense in the U.S., and despite advances in treatments directed at correcting abnormal blood glucose, the development of preventive strategies have lagged.

Hyperglycemia is the major risk factor for development of diabetic microvascular diseases, including cardiomyopathy, nephropathy, retinopathy and peripheral neuropathy [8–12]. Hyperglycemia often develops after the onset of obesity, and intensifies through stages of insulin resistance and hypersecretion, with a slowly progressing loss of pancreatic islet β-cell mass and function. Eventually, the diminished β-cell mass cannot secrete sufficient insulin to support a compromised insulin-dependent glucose uptake in peripheral muscle, and blood sugar levels rise. Intensive treatment of diabetic patients, to lower blood glucose levels to near-normal values, significantly reduces microvascular complications of diabetics. However, in spite of aggressive drug therapy, insulin production in type 2 diabetes patients persistently declines [13]. Importantly, the fundamental feature of cellular oxidative stress and mitochondrial reactive oxygen production is central to the decline in β-cell mass [13–15], and hyperglycemic tissue damage [16–18]. These pathways include the formation of advanced glycation products, glucose metabolism through the polyol pathway, protein kinase C activation and the glucosamine pathway [19]. Such oxidative pathways that mediate hyperglycemic disease provide potential targets for therapeutic intervention.

Previous studies have shown that the widely used over-the-counter analgesic pharmaceutical, acetaminophen (APAP), has strong antioxidant properties in a number of biological systems [20–27]. Therefore, we examined the potential for APAP to intervene in the development of diabetes and obesity, using mouse models of type 1 diabetes and type 2 diabetes.

2. Materials and methods

2.1. Chemicals

All chemicals and reagents were obtained from Sigma–Aldrich Chemical Company (St. Louis, MO) as the highest available grades.

2.2. Animals and treatment

All experiments involving mice were conducted in accordance with the National Institutes of Health standards for care and use of experimental animals and the University of Cincinnati Institutional Animal Care and Use Committee. Female C57BL/6J mice were purchased from Jackson Laboratory (Bar Harbor, ME). Animals were group-housed, maintained on a 12 h light/dark cycle and had access to rodent chow and water *ad libitum*. Mice were matched by initial body weight, and assigned to groups. Mice were allowed *ad libitum* either a normal or a high-fat diet that was pelleted, semipurified and nutritionally complete. The normal diet (AIN-93M, Dyets Inc., Bethlehem, PA) contained 3 g of butter oil and 1 g of soybean oil/100 g diet, supplying 16.12 kJ/g diet, with 1.29 kJ of fat [28]. High-fat diet-fed mice received the AIN-93M diet containing 19 g butter oil and 1 g of soybean oil/100 g diet, supplying 19.34 kJ/g diet, with 7.74 kJ of fat. Both diets contained the same amount of protein, minerals and vitamins [29].

Where indicated, mice were treated with APAP by gavage once per day, between 10 am and 12 noon, at a dose (20 mg APAP/kg/d) that is well tolerated in humans and mice. Measurements were made, or mice were sacrificed, 20–24 h after the last APAP treatment. Streptozotocin (STZ) was dissolved in 10 mM citrate buffer (pH 5.0) and injected i.p. following an 8 h fast. Food was returned and the mice received 10% sucrose in the drinking water for 24 h, as described [30].

2.3. Glucose and glucose tolerance test

Glucose concentration was determined with a handheld glucometer (Ascensia Contour glucometer, Bayer) [29]. Bi-weekly samples of 5 μl blood were applied directly to the glucose strip from 8 h fasted mice to measure fasting levels of blood glucose. Glucose tolerance tests were performed after an 8 h fast. After initial blood glucose determinations, 1.5 mg D-glucose/g body weight was administered by i.p. injection, followed by glucose determinations at 20 min intervals for 120 min. Plasma insulin was measured using a radioimmunoassay employing guinea pig anti-insulin serum with high affinity for rodent insulin [31].

2.3.1. Histopathology

Histological examination was used to ensure that our dosing schedule with APAP was below the toxicity threshold to known target organs, such as liver, kidney and olfactory epithelium [32]. Tissues were examined after 4, 7 and 10 weeks of treatment with APAP, and compared to tissues taken from untreated control mice. Mice were euthanized by carbon dioxide asphyxiation, and target tissues were excised to 10% buffered formalin, then embedded in paraffin and sectioned. Sections (5 μm) for histopathological evaluation were stained with hematoxylin and eosin and evaluated, using light microscopy, by an observer blinded to animal treatment.

2.3.2. Metabolic parameters and body composition

Body weights were measured and food and water consumption were estimated twice weekly. In vivo oxygen consumption and CO_2 release were determined using metabolic chambers. Oxygen consumption was determined as gas

consumed in the presence of soda lime to absorb CO_2. CO_2 release was calculated as gas consumed in the absence minus the presence of soda lime. Feeding efficiency was calculated as the mouse weight gain/kcal of food intake [33]. Body composition was assessed in live, unanesthetized mice by nuclear magnetic resonance (NMR) (EchoMRI; EchoMedical Systems, Houston TX, www.echomri.com). This method provides estimates of total fat tissue, lean tissue (muscle) and water [34–36].

2.3.3. *Parameters of mitochondrial energy coupling and reactive oxygen production*

Mice were killed by carbon dioxide asphyxiation. Liver was excised and mitochondria were isolated, washed and suspended in respiratory buffer (70 mM sucrose, 220 mM mannitol, 0.5 mM EDTA, 2.5 mM KH_2PO_4, 2.5 mM $MgCl_2$, 0.1% bovine serum albumin and 2 mM Hepes, pH 7.4) [37]. Mitochondrial oxygen consumption was measured polarographically with a Clark-type oxygen electrode (Hansatech Instruments, Norfolk, England). Briefly summarized, 0.5 ml of respiratory buffer and 50 mg of mitochondrial protein were equilibrated at 37 °C with stirring. The rate of state 4 respiration (ADP-limited) was determined in the presence of 6 mM succinate. Following the addition of 0.2 mM ADP, the rate of state 3 respiration was measured. The respiratory control ratio (RCR) was calculated as the ratio of states 3:4 respiration. H_2O_2 and superoxide were monitored in freshly prepared mitochondria as luminol (5-amino-2,3-dihydro-1,4-phthalazinedione) or lucigenin (bis-*N*-methylacridinium) chemiluminescence, respectively [37].

The mitochondrial inner membrane potential using the cationic lipophilic dye JC-1 (5,5,6,6-tetrachloro-1,1,3,3-tetraethylbenzimidazolylcarbocyanine iodide) [38], and ATP determinations [39] were assayed as described previously.

2.4. *Statistics*

Statistical significance of the differences between group sample mean values was determined by one-way analysis of variance, followed by the Student–Newman–Kuels test for pairwise comparison of means. Statistics were performed using SigmaStat Statistical Analysis software (SPSS Inc., Chicago, IL).

2.5. *Biohazard precaution*

STZ is toxic. All personnel were instructed in safe handling procedures, including wearing laboratory coats, gloves and masks.

3. Results

The histological appearance of liver, kidney, and olfactory mucosa from APAP-treated mice was indistinguishable from tissues from vehicle-treated controls (results not shown), indicating that APAP was not toxic at the dosage used. Treatment with STZ caused a dose-dependent increase in fasting blood glucose (FBG) levels (Fig. 1, left panel). APAP pretreatment plus daily APAP treatment caused FBG to be lower in STZ-treated mice, even at a high dosage of 200 mg STZ/kg body weight. The effect of APAP was not solely the result of protection from initial damage by STZ, as demonstrated by the data presented in the right panels of Fig. 1 (the results of two separate trials are shown). FBG rose progressively in mice treated only with 175 mg STZ/kg. APAP treatment reversed the steady increase in FBG produced by STZ. However, when APAP was discontinued at day-6, FBG began to rise again. This cycle was repeated. Shortly after APAP treatment was begun again at day-10, FBG began to fall.

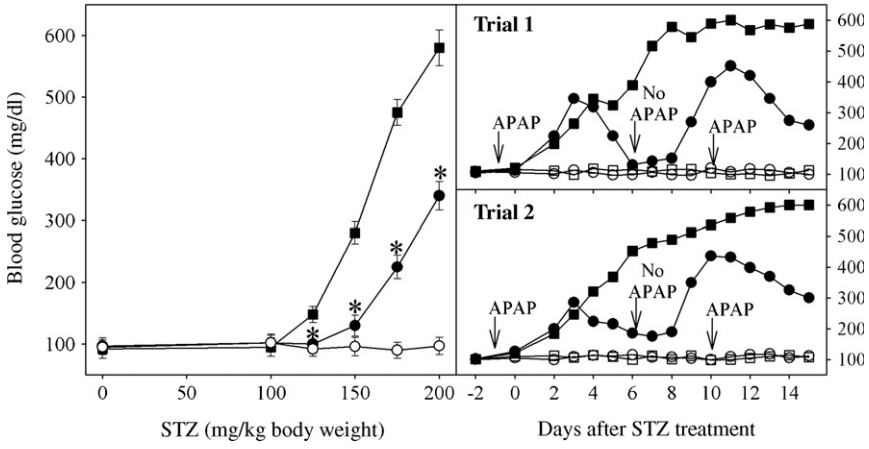

Fig. 1 – APAP lowers the increase in fasting blood glucose produced by STZ. Mice received streptozotocin (STZ) on day-0 (closed symbols), or they received vehicle (open symbols). Mice were gavaged daily with 20 mg APAP/kg body weight (circles), or with the equivalent volume of isotonic saline vehicle (squares). For data in the left panel, blood glucose was monitored on day-12, following an 8 h fast. Mean values ± S.E.M. (N = 4) are shown for each group. *Significantly lower mean value than the mean obtained from mice treated with STZ alone. $P < 0.01$. For data in the right panels, the STZ dosage was 175 mg/kg body weight, and APAP was administered from day-minus 1 to day-6, and from day-10 to day-14. Mean values (N = 2) are shown for each of two trials.

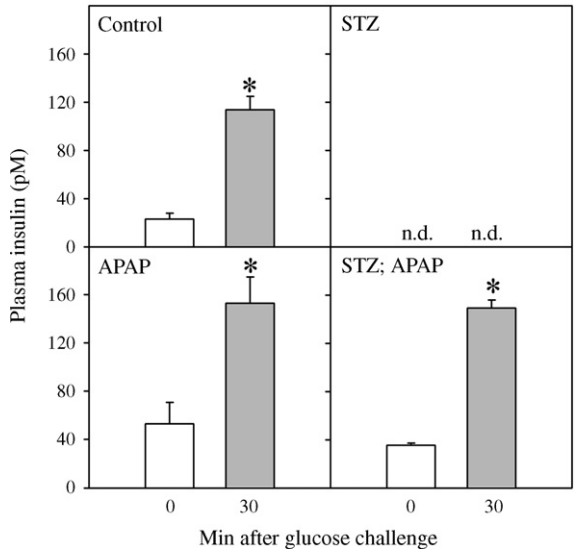

Fig. 2 – Plasma insulin levels in STZ mice. Mice fed a normal diet were treated with 200 mg STZ/kg BW on day 0 (right panels). In addition, mice received daily gavage with 20 mg APAP/kg body weight, starting 7 days before STZ (lower panels). The bars represent mean serum insulin levels ± S.E.M. (N = 4) in mice before (open) and 30 min after (shaded) a glucose challenge. n.d. indicates that insulin levels were below the level of detection (5 pM). *Significantly higher mean value than basal mean obtained prior to the glucose challenge ($P < 0.01$).

In order to gain a more complete understanding how APAP contributes to improved glucose metabolism, plasma insulin levels were measured for mice treated with STZ, before and after i.p. glucose (Fig. 2). In untreated mice fed a normal diet, plasma insulin levels increased at 20 min following a glucose challenge (top left panel). APAP did not significantly change the response of insulin to the glucose challenge (bottom left panel). In mice treated 12 days previously with 200 mg STZ/kg body weight, fasting basal and glucose-challenged levels of plasma insulin were not detectable (<5 pM) (top right panel). When APAP was administered prior to STZ and daily thereafter, basal and glucose-challenged levels of plasma insulin were completely normalized (bottom right panel).

Although initial body weights for mice fed a high-fat diet for 10 weeks were matched to normal chow-fed controls, high-fat diet-fed mice gained weight at a greater rate and developed changes in body composition, with higher percentages of fat and lower percentages of lean (muscle) tissue and water content (Fig. 3). However, the actual weights of muscle and water did not change in mice receiving the high-fat diet (Table 2), with most of the increase in body weight due to fat accumulation. Animals treated with APAP during high-fat feeding exhibited only 1/3 of the gain in percentage of body fat seen in untreated mice.

Animals fed the high-fat diet had normal FBG levels (Fig. 4, left panel), but displayed impaired glucose tolerance following an i.p. injection of 1.5 mg glucose/g body weight (Fig. 4, right panels). For high-fat diet mice, blood glucose area-under-the-curve (AUC = 24,690 min mg/dl) was significantly higher than that of mice fed a normal diet (19,370 min mg/dl). Pretreatment, and subsequent daily treatment, with APAP reduced blood glucose AUCs for normal and high-fat diet mice to 15,170 min mg/dl and 14,600 min mg/dl, respectively, thus improving glucose tolerance for mice fed a high-fat diet. Furthermore, mice fed the high-fat diet displayed fasting hyperinsulemia (Fig. 5), but high-fat diet-fed mice treated with APAP had normal basal insulin levels (Fig. 5, bottom right panel).

In order to evaluate whether the changes in body fat composition are the result of changes in systemic energy flow, we measured parameters of energy consumption and utilization (Table 1). Although mice on the high-fat diet gained weight about 50% more rapidly than mice on the normal diet, APAP had no effect on the rate of weight gain with either diet. Interestingly, the mice consumed less food by weight of the high-fat diet, yet the energy consumed was the same on both diets. APAP did not affect food consumption, and caused no significant effects on a number of metabolic parameters, including oxygen consumption, CO_2 expiration, energy efficiency (metabolism per unit of food consumed) and feeding efficiency (conversion of food to body mass). APAP also had no effect on respiratory quotient, indicative that the proportions of fat, carbohydrate and protein utilized for intermediary metabolism were unchanged.

The production of insulin by β-cells of the pancreatic islets is central to the regulation of blood glucose, and mitochondrial oxidative stress is involved in the destruction of β-cells by both STZ and excess body fat. Since APAP has been shown previously to inhibit oxidative stress in other biological systems, we evaluated the ability of APAP to quench the production of mitochondria-derived reactive oxygen. In isolated liver mitochondria, APAP slightly depressed state 3 respiration and slightly stimulated state 4 (ADP-limited) respiration (Fig. 6, top panel), such that the respiratory control ratio (RCR; state 3/state 4) was significantly reduced (Fig. 5, second panel, open circles), suggesting that APAP partially uncoupled mitochondrial ATP synthesis from respiration. A more precise indicator of coupling, however, is the ratio of ATP synthesized to oxygen consumed, which was not reduced by APAP (Fig. 6, bottom panel, closed squares). Most important for sustaining the viability of mitochondria are membrane potential (Fig. 6, second panel, closed squares) and the rate of ATP production (Fig. 6, bottom panel, open circles), which were very slightly decreased by APAP, and only at concentrations in the 100 μM range. In contrast to mitochondrial parameters that required high APAP concentrations to achieve minimal effect, APAP was a potent inhibitor of succinate-stimulated H_2O_2 and superoxide production under ADP-limited conditions (Fig. 6, third panel), with IC_{50} values for APAP inhibition of about 0.4 and 1.5 μM, respectively.

In order to determine the response of mitochondria to APAP treatment in vivo, mice were fed either a normal or a high-fat diet for 10 weeks, and gavaged daily with either APAP or vehicle. Mitochondria were isolated from the livers of mice after sacrifice. Mice fed a high-fat diet exhibited higher rates of succinate-dependent state 4 (ADP-limited) respiration, with no change in state 3 respiration (Fig. 7). The resulting decrease in RCR indicates that liver mitochondria from mice fed a high-fat diet were partially uncoupled. These mice exhibited lower rates of succinate-stimulated H_2O_2 production. Although

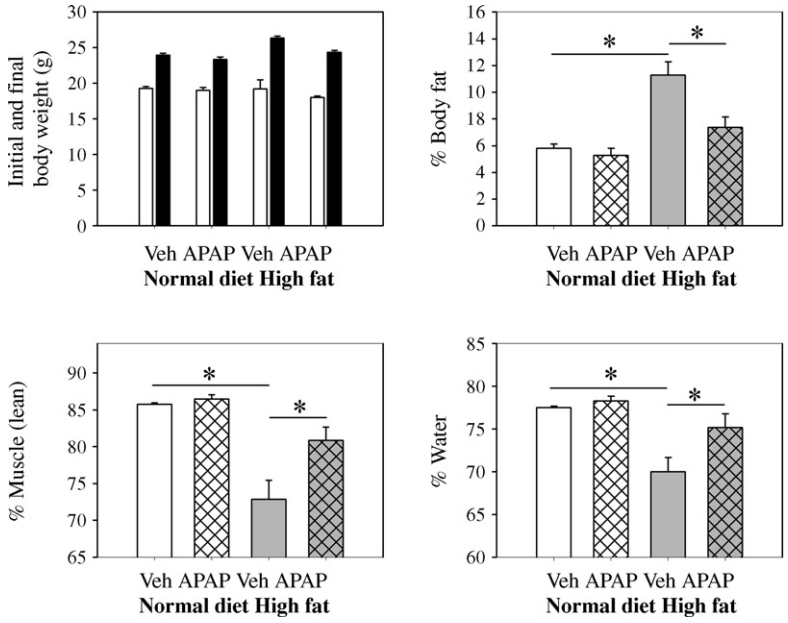

Fig. 3 – Effect of high-fat diet and APAP on body composition. Mice were fed a normal diet, or a high-fat diet for 10 weeks. Mice were gavaged daily with 20 mg APAP/kg body weight, or with the equivalent volume of isotonic saline vehicle, beginning 7 days before changing to a high-fat diet. The bars represent mean values for the parameters indicated on the abscissas ± S.E.M. (N = 4). In the upper left panel, initial (open bars) and final (black bars) body weights are shown. For each of the other panels, body fat, muscle and water are displayed as percentages of body weight. The actual weight of body fat, lean muscle and water, independent of body weight, are shown in Table 2. *Significantly different mean values between the indicated groups (P < 0.01).

treatment with APAP in vivo about 1 day prior to sacrifice did not affect mitochondrial state 3 or state 4 respiration, APAP decreased the rates of H_2O_2 production by about a third, in mice fed either a normal or a high-fat diet.

4. Discussion

The inability of the β-cells of the pancreas to secrete the necessary amount of insulin to maintain blood glucose homeostasis is the hallmark of both type 1 diabetes and type 2 diabetes. In the type 2 diabetes prediabetic state associated with glucose intolerance, loss of insulin homeostasis is a major contributing factor in the progression toward frank diabetes. We have shown that in STZ-treated mice and in glucose intolerant high-fat-fed mice, APAP improves β-cell function and glucose homeostasis. This effect of APAP is associated with changes in mitochondrial respiration and diminished production of reactive oxygen. These findings demonstrate that toxic and metabolic

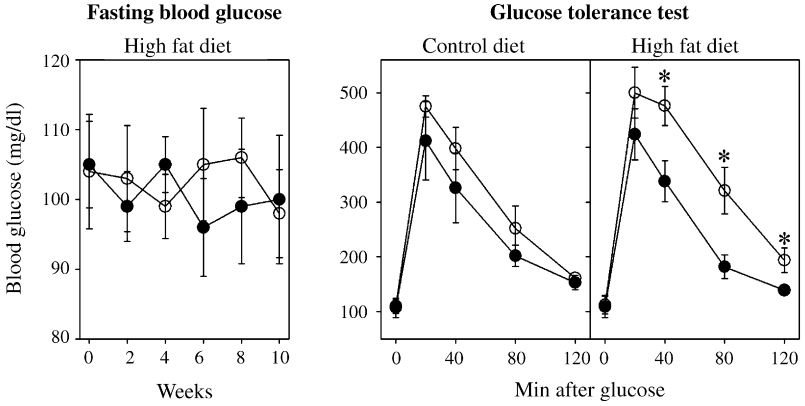

Fig. 4 – APAP protects against hyperglycemia in mice fed a high-fat diet. Mice were gavaged daily with 20 mg APAP/kg body weight (closed circles), or with the equivalent volume of isotonic saline vehicle (open circles), beginning 7 days before changing to a high-fat diet, where indicated. After 10 weeks, mice were given a glucose tolerance test, and blood glucose determined at 20 min intervals for 120 min. Mean values ± S.E.M. (N = 4) are shown for each group. *Significantly greater mean value than from each of the other groups (P < 0.01).

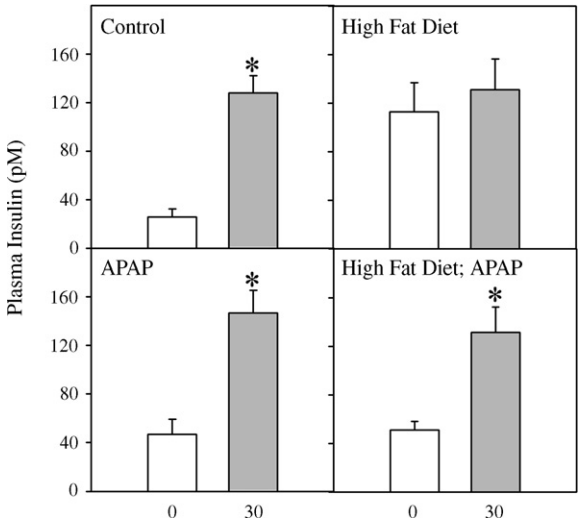

Fig. 5 – Plasma insulin levels in high-fat diet mice. Mice were fed a normal diet (left panels), or a high-fat diet for 10 weeks (right panels). Mice received daily gavage with 20 mg APAP/kg body weight, starting 1 week before initiating the high-fat diet (lower panels). The bars represent mean serum insulin levels ± S.E.M. (N = 4) in mice before (open) and 30 min after (shaded) a glucose challenge. *Significantly higher mean value than mean obtained from mice just before the glucose challenge (P < 0.01).

stressors on the β-cell share common mechanisms that can be blocked by APAP.

Type 1 diabetes is most often modeled in rodents by chemical destruction of insulin-producing β-cells of the pancreatic islets, using STZ [40]. Rapid onset of hyperglycemia (blood glucose levels of about 250 mg/dl within 48 h) is followed within weeks by diabetic microvascular diseases that include cardiovascular disease, nephropathy, retinopathy and neuropathy [41–44]. In the experiments described here, the increase in fasting glycemia with increasing dosages of STZ can be logically attributed to greater degrees of β-cell injury. The absence of measurable insulin in mice receiving a high dose of STZ, before and after a glucose challenge, and the ability of mice treated with both STZ and APAP to respond to a glucose challenge, suggests that APAP protects from loss of β-cell function.

In C57BL/6J mice, a high-fat diet-induces type 2 diabetes [45], a model which is highly relevant for the current crisis regarding increase in obesity in our society. For this reason we utilized this animal model for APAP intervention studies. A high-fat diet leads to insulin resistance, impaired glucose control, an increase in body fat and dyslipidemia, and eventually fasting hyperglycemia [4,5,45,46]. It is important to note, however, that even transient hyperglycemia can produce oxidative tissue damage that may result in cell death [47]. Thus, insulin resistance and impaired glucose control pose substantial risks for development of hyperglycemia-derived pathology. The mice in this study that were fed the high-fat diet had normal levels of FBG, but higher than normal levels of fasting blood insulin, consistent with insulin resistance. After 10 weeks on the high-fat diet, these mice are in a pre-diabetic metabolic state and would eventually develop frank diabetes associated with elevated FBG [45]. Hyperinsulemia in association with increased amounts of body fat is well-described in C57BL/6J mice fed a high-fat diet [45]. In these mice, the elevated fasting insulin levels, and the inability of i.p. glucose to further increase blood insulin, is indicative of diet-induced β-cell dysfunction. Thus, both STZ and a high-fat diet produce β-cell dysfunction, with significant protection by APAP. These findings are compatible with STZ and the high-fat diet operating via a common destructive pathway that is susceptible to intervention by APAP.

Because hyperglycemia is associated with perturbed mitochondrial function [48], we examined mitochondrial parameters of respiration and reactive oxygen formation. Directly adding APAP to isolated liver mitochondria somewhat reduced the respiratory control ratio (RCR; state 3/state 4), suggesting that APAP partially uncoupled mitochondrial ATP synthesis from respiration. Via this partial uncoupling pathway, APAP lowers mitochondrial membrane potential sufficiently to inhibit the production of reactive oxygen, similar to the effect of Ca^{2+} at low concentrations [49]. This appears to be the mechanism responsible for the decrease in H_2O_2 production in mice fed a high-fat diet. In the high-fat diet mice, higher levels of free fatty acids such as oleate and linoleate may increase inner membrane permeability via opening the

Table 1 – Systemic energy parameters of APAP treatment

Parameter	Control diet		High-fat diet	
(units as shown)	Vehicle	APAP	Vehicle	APAP
Weight gain (% BW change/week)	2.4 ± 0.2	2.3 ± 0.2	3.7 ± 0.3*	3.5 ± 0.4*
Food consumed (g/d/100 g BW)	15.4 ± 1.2	15.9 ± 1.1	12.4 ± 0.9*	12.6 ± 0.8*
Food consumed (kJ/d/100 g BW)	248 ± 19	256 ± 18	240 ± 15	244 ± 13
O_2 (ml/h/kg BW)	2995 ± 154	2809 ± 137	2680 ± 212	2340 ± 138
O_2 (kJ/h/100 g BW)	5.7 ± 0.3	5.3 ± 0.3	5.1 ± 0.4	4.5 ± 0.3
CO_2 (ml/h/kg BW)	2426 ± 134	2311 ± 149	2013 ± 114	1798 ± 74
RQ (CO_2/O_2)	0.81 ± 0.04	0.82 ± 0.02	0.755 ± 0.02	0.772 ± 0.3
Energy efficiency (O_2/food)	0.55 ± 0.03	0.50 ± 0.02	0.51 ± 0.04	0.44 ± 0.04
Feeding efficiency (mg BW gain/kJ food)	1.38 ± 0.06	1.28 ± 0.07	2.20 ± 0.09	2.05 ± 0.08

These parameters were measured in live mice. Mean values ± S.E.M. (N = 4) are shown for each group. *Significantly different mean value than the corresponding mean from mice with or without APAP treatment. $P < 0.05$.

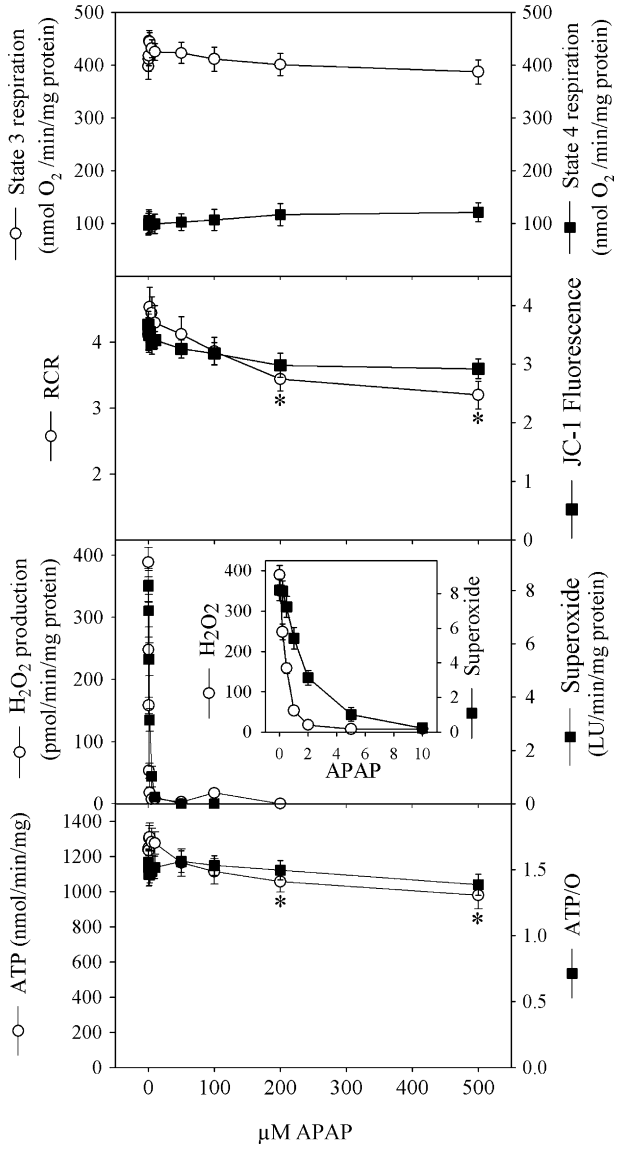

Fig. 6 – Direct effect of APAP on mitochondrial oxygen metabolism. Mitochondria were prepared from livers of 8 h fasted mice fed a normal diet. APAP was added directly to the mitochondria at the concentrations indicated. Various parameters of mitochondrial activity were assayed as described in Section 2. Shown are mean values for the parameters indicated ± S.E.M. (N = 4). *Significantly different mean value than obtained in the absence of APAP (P < 0.05).

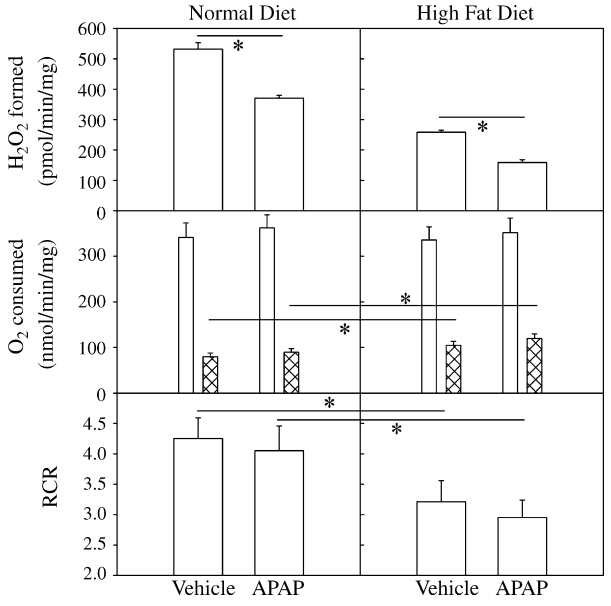

Fig. 7 – Effect of treating mice with APAP on mitochondrial oxygen metabolism. Mice were fed a normal diet (left panels), or a high-fat diet (right panels) for 10 weeks. Mice were gavaged daily with 20 mg APAP/kg body weight, or with the equivalent volume of isotonic saline vehicle, beginning 7 days before changing to a high-fat diet. Mitochondria were prepared from livers of 8 h fasted mice, and parameters of mitochondrial activity were assayed. Oxygen consumed was measured as state 3 respiration (open bars) or state 4 ADP-limited respiration (hatched bars). Shown are mean values for the parameters indicated ± S.E.M. (N = 4). *Significantly different mean values between the indicated groups (P < 0.05).

permeability transition pore, resulting in a lower membrane potential associated with decreased succinate-dependent reactive oxygen production [49]. Although the lower RCR observed when APAP is added to mitochondria suggests this possibility, it is unlikely to be a major contributor, for several reasons. First, the concentration of APAP to produce the change in RCR is relatively high. Second, the ratio of ATP synthesized to oxygen consumed (ATP/O) is a more precise indicator of coupling [49], and this parameter is not significantly changed by APAP. Similarly, APAP did not significantly reduce the mitochondrial membrane potential. Third,

Table 2 – Actual weights for body fat, lean muscle and water

Component	Control diet		High-fat diet	
(g)	Vehicle	APAP	Vehicle	APAP
Body fat	1.39 ± 0.07	1.23 ± 0.13	2.97 ± 0.26*	1.79 ± 0.20*
Muscle	20.5 ± 0.2	20.2 ± 3	19.3 ± 0.7	19.7 ± 0.5
Water	18.6 ± 0.1	18.3 ± 0.1	18.4 ± 0.4	18.3 ± 0.4

Mice were fed a normal diet or a high-fat diet for 10 weeks. Mice were gavaged daily with 20 mg APAP/kg body weight, or with the equivalent volume of isotonic saline vehicle, beginning 7 days before changing to a high-fat diet. The table shows mean values for the parameters indicated ± S.E.M. (N = 4). The percentages body fat, lean muscle and water, based on body weight, are shown in Fig. 3. *Significantly different mean values between the indicated groups (P < 0.01).

the increase in oxygen consumption in vivo, expected if there is partial mitochondrial uncoupling (increase in mitochondrial state 4 respiration), is not observed.

A more attractive hypothesis for the ability of APAP to inhibit mitochondrial-derived reactive oxygen levels is that, in vitro and in vivo, APAP is acting directly as a phenolic radical scavenger, similar to α-tocopherol. This possibility is suggested from a number of studies demonstrating the antioxidant properties of APAP in various biological systems. In human erythrocyte membranes, APAP inhibited H_2O_2-initiated lipid peroxidation [27]. APAP also inhibited low density lipoprotein oxidation and decreases in hydroperoxide content of low density lipoproteins in mice [23]. In the ischemic guinea pig heart, APAP decreased the release of hydroxyl radicals and peroxynitrite, decreased protein oxidation, decreased myocardial damage from H_2O_2 [25,26], and decreased peroxynitrite-initiated activation of matrix metalloproteinase-2, which is involved in ischemia-reperfusion myocardial injury [21]. In rodent brain, APAP inhibited amyloid beta-peptide induced oxidative stress in rat neurons, including lipid peroxidation and peroxide accumulation [24]. APAP also inhibited quinolinic acid-mediated superoxide production and lipid peroxidation in rat hippocampus [20], and inhibited cyanide-induced superoxide production and lipid peroxidation in rat brain [22].

Theoretically, the antioxidant effects of APAP could result in part from a direct action of APAP on protecting the insulin-producing β-cells from oxidative stress. A rough calculation shows that 20 mg APAP, evenly distributed in one kg body weight at 77% water, would have a concentration of 172 μM. If we assume that APAP has a biological first order half-life of about 1.5 h [50,51], then after 6 half-life decays (9 h), the plasma concentration would be 2.7 μM. The IC_{50} values for H_2O_2 and superoxide by APAP in isolated mitochondria were about 0.4 and 1.5 μM, respectively. This amount of time could be sufficient to protect, in part, against STZ β-cell toxicity, or against the oxidative stress pathways associated with increased body fat. This prediction was confirmed when we examined mitochondria from mice approximately 22 h after the last APAP treatment. For APAP-treated mice fed either a normal or a high-fat diet, succinate-dependent H_2O_2 production was lower than in liver mitochondria from vehicle-treated controls. This effect of APAP was not associated with a change in mitochondrial energy coupling.

Diabetes is associated with a multitude of debilitating health effects including microvascular diseases (nephropathy, cardiovascular disease, peripheral neuropathy), and is associated with obesity and metabolic diseases. This study has shown that APAP, a widely used over-the-counter drug, has the potential to ameliorate some of these untoward health effects by slowing and/or preventing the loss of β-cell mass and the ability to secrete insulin. The dosage of APAP utilized in this study (20 mg/kg/d), approximately equivalent to 2.5 extra-strength tablets of APAP per day in humans, is well within the dose range used routinely and safely by humans. Thus, APAP may provide an inexpensive and safe component in the prevention and treatment of diabetes.

Acknowledgements

This study was supported in part by a research grant from McNeil Consumer Healthcare. The Obesity Research Center at the University of Cincinnati is supported in part by Procter & Gamble. We thank Dr. Randy Seeley for scientific comments and encouragement. We especially thank Kathy LaDow, and also Jennifer Schurdak and Kay Ellis, for their expert technical assistance.

REFERENCES

[1] Allison DB, Fontaine KR, Manson JE, Stevens J, VanItallie TB. Annual deaths attributable to obesity in the United States. JAMA 1999;282:1530–8.
[2] U.S. Department of Health and Human Services. The Surgeon General's call to action to prevent and decrease overweight and obesity. http://www.surgeongeneral.gov/topics/obesity/calltoaction/CalltoAction.pdf. 2001. Washington, DC, U.S. Government Printing Office.
[3] Fontaine KR, Redden DT, Wang C, Westfall AO, Allison DB. Years of life lost due to obesity.. JAMA 2003;289:187–93.
[4] Smith Jr SC. Multiple risk factors for cardiovascular disease and diabetes mellitus. Am J Med 2007;120:S3–11.
[5] Rader DJ. Effect of insulin resistance, dyslipidemia, and intra-abdominal adiposity on the development of cardiovascular disease and diabetes mellitus. Am J Med 2007;120:S12–8.
[6] Ohgami N, Nagai R, Ikemoto M, Arai H, Miyazaki A, Hakamata H, et al. CD36, serves as a receptor for advanced glycation endproducts (AGE). J Diabetes Complications 2002;16:56–9.
[7] Thornalley PJ. Cell activation by glycated proteins. AGE receptors, receptor recognition factors and functional classification of AGEs. Cell Mol Biol 1998;44:1013–23.
[8] Goralski KB, Sinal CJ. Type 2 diabetes and cardiovascular disease: getting to the fat of the matter. Can J Physiol Pharmacol 2007;85:113–32.
[9] Susztak K, Raff AC, Schiffer M, Bottinger EP. Glucose-induced reactive oxygen species cause apoptosis of podocytes and podocyte depletion at the onset of diabetic nephropathy. Diabetes 2006;55:225–33.
[10] Beisswenger PJ, Drummond KS, Nelson RG, Howell SK, Szwergold BS, Mauer M. Susceptibility to diabetic nephropathy is related to dicarbonyl and oxidative stress. Diabetes 2005;54:3274–81.
[11] Duby JJ, Campbell RK, Setter SM, White JR, Rasmussen KA. Diabetic neuropathy: an intensive review. Am J Health Syst Pharm 2004;61:160–73.
[12] Valeri C, Pozzilli P, Leslie D. Glucose control in diabetes. Diab Metab Res Rev 2004;20(Suppl. 2):S1–8.
[13] Robertson RP, Harmon J, Tran PO, Poitout V. Beta-cell glucose toxicity, lipotoxicity, and chronic oxidative stress in type 2 diabetes. Diabetes 2004;53(Suppl. 1):S119–24.
[14] Robertson RP, Harmon J, Tran PO, Tanaka Y, Takahashi H. Glucose toxicity in beta-cells: type 2 diabetes, good radicals gone bad, and the glutathione connection. Diabetes 2003;52:581–7.
[15] Robertson RP. Chronic oxidative stress as a central mechanism for glucose toxicity in pancreatic islet beta cells in diabetes. J Biol Chem 2004;279:42351–4.
[16] Nishikawa T, Edelstein D, Du XL, Yamagishi S, Matsumura T, Kaneda Y, et al. Normalizing mitochondrial superoxide production blocks three pathways of hyperglycaemic damage. Nature 2000;404:787–90.

[17] Pennathur S, Heinecke JW. Mechanisms for oxidative stress in diabetic cardiovascular disease. Antioxid Redox Signal 2007;9:955–69.
[18] Shah S, Iqbal M, Karam J, Salifu M, McFarlane SI. Oxidative stress, glucose metabolism, and the prevention of type 2 diabetes: pathophysiological insights. Antioxid Redox Signal 2007;9:911–29.
[19] Hammes HP, Du X, Edelstein D, Taguchi T, Matsumura T, Ju Q, et al. Benfotiamine blocks three major pathways of hyperglycemic damage and prevents experimental diabetic retinopathy. Nat Med 2003;9:294–9.
[20] Maharaj H, Maharaj DS, Daya S. Acetylsalicylic acid and acetaminophen protect against oxidative neurotoxicity. Metab Brain Dis 2006;21:189–99.
[21] Rork TH, Hadzimichalis NM, Kappil MA, Merrill GF. Acetaminophen attenuates peroxynitrite-activated matrix metalloproteinase-2-mediated troponin I cleavage in the isolated guinea pig myocardium. J Mol Cell Cardiol 2006;40:553–61.
[22] Maharaj DS, Saravanan KS, Maharaj H, Mohanakumar KP, Daya S. Acetaminophen and aspirin inhibit superoxide anion generation and lipid peroxidation, and protect against 1-methyl-4-phenyl pyridinium-induced dopaminergic neurotoxicity in rats. Neurochem Int 2004;44:355–60.
[23] Chou TM, Greenspan P. Effect of acetaminophen on the myeloperoxidase-hydrogen peroxide-nitrite mediated oxidation of LDL. Biochim Biophys Acta 2002;1581:57–63.
[24] Bisaglia M, Venezia V, Piccioli P, Stanzione S, Porcile C, Russo C, et al. Acetaminophen protects hippocampal neurons and PC12 cultures from amyloid beta-peptides induced oxidative stress and reduces NF-kappaB activation. Neurochem Int 2002;41:43–54.
[25] Merrill GF. Acetaminophen and low-flow myocardial ischemia: efficacy and antioxidant mechanisms. Am J Physiol Heart Circ Physiol 2002;282:H1341–9.
[26] Merrill GF, Goldberg E. Antioxidant properties of acetaminophen and cardioprotection. Basic Res Cardiol 2001;96:423–30.
[27] Orhan H, Sahin G. In vitro effects of NSAIDS and paracetamol on oxidative stress-related parameters of human erythrocytes. Exp Toxicol Pathol 2001;53:133–40.
[28] Reeves PG, Nielsen FH, Fahey Jr GC. AIN-93 purified diets for laboratory rodents: final report of the American Institute of Nutrition ad hoc writing committee on the reformulation of the AIN-76A rodent diet. J Nutr 1993;123:1939–51.
[29] Woods SC, Seeley RJ, Rushing PA, D'Alessio D, Tso P. A controlled high-fat diet induces an obese syndrome in rats. J Nutr 2003;133:1081–7.
[30] Brosius F. Low-dose streptozotocin induction protocol (mouse). In: Animal models of diabetic complications consortium protocols. Ann Arbor: University of Michigan Medical Center; 2003. pp. 1–3.
[31] Elder DA, Prigeon RL, Wadwa RP, Dolan LM, D'Alessio DA. Beta-cell function, insulin sensitivity, and glucose tolerance in obese diabetic and nondiabetic adolescents and young adults. J Clin Endocrinol Metab 2006;91:185–91.
[32] Genter MB, Liang HC, Gu J, Ding X, Negishi M, McKinnon RA, et al. Role of CYP2A5 and 2G1 in acetaminophen metabolism and toxicity in the olfactory mucosa of the Cyp1a2(−/−) mouse. Biochem Pharmacol 1998;55:1819–26.
[33] Almind K, Kahn CR. Genetic determinants of energy expenditure and insulin resistance in diet-induced obesity in mice. Diabetes 2004;53:3274–85.
[34] Tinsley FC, Taicher GZ, Heiman ML. Evaluation of a quantitative magnetic resonance method for mouse whole body composition analysis. Obes Res 2004;12:150–60.
[35] Taicher GZ, Tinsley FC, Reiderman A, Heiman ML. Quantitative magnetic resonance (QMR) method for bone and whole-body-composition analysis. Anal Bioanal Chem 2003;377:990–1002.
[36] Clegg DJ, Brown LM, Woods SC, Benoit SC. Gonadal hormones determine sensitivity to central leptin and insulin. Diabetes 2006;55:978–87.
[37] Senft AP, Dalton TP, Nebert DW, Genter MB, Puga A, Hutchinson RJ, et al. Mitochondrial reactive oxygen production is dependent on the aromatic hydrocarbon receptor. Free Radic Biol Med 2002;33:1268–78.
[38] Shen D, Dalton TP, Nebert DW, Shertzer HG. Glutathione redox state regulates mitochondrial reactive oxygen production. J Biol Chem 2005;280:25305–12.
[39] Senft AP, Dalton TP, Nebert DW, Genter MB, Hutchinson RJ, Shertzer HG. Dioxin increases reactive oxygen production in mouse liver mitochondria. Toxicol Appl Pharmacol 2002;178:15–21.
[40] Liu K, Paterson AJ, Chin E, Kudlow JE. Glucose stimulates protein modification by O-linked GlcNAc in pancreatic beta cells: linkage of O-linked GlcNAc to beta cell death. Proc Natl Acad Sci USA 2000;97:2820–5.
[41] Genter MB, Amarnath V, Moody MA, Anthony DC, Anderson CW, Graham DG. Pyrrole oxidation and protein cross-linking as necessary steps in the development of gamma-diketone neuropathy. Chem Res Toxicol 1988;1:179–85.
[42] Chow FY, Nikolic-Paterson DJ, Ozols E, Atkins RC, Rollin BJ, Tesch GH. Monocyte chemoattractant protein-1 promotes the development of diabetic renal injury in streptozotocin-treated mice. Kidney Int 2006;69:73–80.
[43] Schmeichel AM, Schmelzer JD, Low PA. Oxidative injury and apoptosis of dorsal root ganglion neurons in chronic experimental diabetic neuropathy. Diabetes 2003;52:165–71.
[44] Obrosova IG, Li F, Abatan OI, Forsell MA, Komjati K, Pacher P, et al. Role of poly(ADP-ribose) polymerase activation in diabetic neuropathy. Diabetes 2004;53:711–20.
[45] Surwit RS, Kuhn CM, Cochrane C, McCubbin JA, Feinglos MN. Diet-induced type II diabetes in C57BL/6J mice. Diabetes 1988;37:1163–7.
[46] Ikemoto S, Thompson KS, Takahashi M, Itakura H, Lane MD, Ezaki O. high-fat diet-induced hyperglycemia: prevention by low level expression of a glucose transporter (GLUT4) minigene in transgenic mice. Proc Natl Acad Sci USA 1995;92:3096–9.
[47] Vincent AM, McLean LL, Backus C, Feldman EL. Short-term hyperglycemia produces oxidative damage and apoptosis in neurons. FASEB J 2005;19:638–40.
[48] Lee HK, Park KS, Cho YM, Lee YY, Pak YK. Mitochondria-based model for fetal origin of adult disease and insulin resistance. Ann NY Acad Sci 2005;1042:1–18.
[49] Shertzer HG, Genter MB, Shen D, Nebert DW, Chen Y, Dalton TP. TCDD decreases ATP levels and increases reactive oxygen production through changes in mitochondrial F(0)F(1)-ATP synthase and ubiquinone. Toxicol Appl Pharmacol 2006;217:363–74.
[50] Kulkarni SG, Pegram AA, Smith PC. Disposition of acetaminophen and indocyanine green in cystic fibrosis-knockout mice. AAPS PharmSci 2000;2:E18.
[51] Gu J, Cui H, Behr M, Zhang L, Zhang QY, Yang W, et al. In vivo mechanisms of tissue-selective drug toxicity: effects of liver-specific knockout of the NADPH-cytochrome P450 reductase gene on acetaminophen toxicity in kidney, lung, and nasal mucosa. Mol Pharmacol 2005;67:623–30.